HHS Public Access

Author manuscript

Oncogene. Author manuscript; available in PMC 2020 October 15.

Published in final edited form as:

Oncogene. 2013 May 30; 32(22): 2726–2738. doi:10.1038/onc.2012.301.

CD97 amplifies LPA receptor signaling and promotes thyroid cancer progression in a mouse model

Y Ward[1,9], **R Lake**[1,9], **PL Martin**[1], **K Killian**[2], **P Salerno**[3], **T Wang**[4], **P Meltzer**[2], **M Merino**[5], **S-y Cheng**[6], **M Santoro**[7], **G Garcia-Rostan**[8], **K Kelly**[1]

[1]Cell and Cancer Biology Branch, Center for Cancer Research, NCI, Bethesda, MD, USA

[2]Genetics Branch, Center for Cancer Research, NCI, Bethesda, MD, USA

[3]Medical Oncology Branch, Center for Cancer Research, NCI, Bethesda, MD, USA

[4]The Wistar Institute, Philadelphia, PA, USA

[5]Laboratory of Pathology, Center for Cancer Research, NCI, Bethesda, MD, USA

[6]Laboratory of Molecular Biology, Center for Cancer Research, NCI, Bethesda, MD, USA

[7]Dipartimento di Biologia e Patologia Cellulare e Molecolare, Universita' Federico II, Naples, Italy

[8]Institute of Biology and Molecular Genetics, Valladolid University, Spanish Research Council, Valladolid, Spain.

[9]These authors contributed equally to this work.

Abstract

CD97, a member of the adhesion family of G-protein-coupled receptors (GPCRs), complexes with and potentiates lysophosphatidic acid (LPA) receptor signaling to the downstream effector RHOA. We show here that CD97 was expressed in a majority of thyroid cancers but not normal thyroid epithelium and that the level of CD97 expression was further elevated with progression to poorly differentiated and undifferentiated carcinoma. Intratumoral progression also showed that CD97 expression correlates with invasiveness and dedifferentiation. To determine the functional role of CD97, we produced a transgenic model of thyroglobulin promoter-driven CD97 expression. Transgenic CD97 in combination with *Thrb*^{PV}, an established mouse model of thyroid follicular cell carcinogenesis, significantly increased the occurrence of vascular invasion and lung metastasis. Expression of transgenic CD97 in thyroid epithelium led to elevated ERK phosphorylation and increased numbers of Ki67 + cells in developing tumors. In addition, tumor cell cultures derived from CD97 transgenic as compared with non-transgenic mice demonstrated enhanced, constitutive and LPA-stimulated ERK activation. In human thyroid cancer cell lines, CD97 depletion reduced RHO-GTP and decreased LPA-stimulated invasion but not EGF-stimulated invasion, further suggesting that CD97 influences an LPA-associated mechanism of

Correspondence: Dr K Kelly, Cell and Cancer Biology Branch, Center for Cancer Research, NCI, Building 37 Room 1068, Bethesda, MD 20892, USA. kellyka@mail.nih.gov.

CONFLICT OF INTEREST

The authors declare no conflict of interest.

Supplementary Information accompanies the paper on the Oncogene website (http://www.nature.com/onc)

progression. Consistent with the above, CD97 expression in human thyroid cancers correlated with LPA receptor and markers of aggressiveness including Ki67 and pAKT. This study shows an autonomous effect of CD97 on thyroid cancer progression and supports the investigation of this GPCR as a therapeutic target for these cancers.

Keywords

CD97; LPAR; thyroid cancer; metastasis; vascular invasion; anaplastic

INTRODUCTION

Thyroid cancer originating in follicular cells accounts for ~90% of all endocrine malignancies.[1] Sporadic thyroid follicular cell tumorigenesis (TFCT) encompasses several histopathological tumor types with different degrees of differentiation and aggressiveness. There is compelling histopathogenetic evidence supporting a stepwise progression from indolent, differentiated thyroid carcinomas (DTCs) of papillary (PTC) or follicular (FTC) type to highly aggressive and poorly differentiated (PDC) and undifferentiated (UC) thyroid carcinomas.[1–4] It is estimated that, in up to 30% of DTC, dedifferentiation and progression to PDC or UC may occur.[5] The unfavorable clinical outcome of PDCs is intermediate between the dismal prognosis of UCs and the mild clinical course for PTCs and minimally invasive FTCs.[2–4] Although UC accounts for less than 2–5% of thyroid cancers, about one-third of deaths due to thyroid cancer are attributed to UC as there are no effective treatments.[6,7]

In the last 20 years, there has been significant improvement in the understanding of the molecular genetics underlying the development of TFCT. However, there is a need to understand the cellular biochemical mechanisms governing transformation of indolent, morphologically indistinguishable PTCs or minimally invasive FTCs to aggressive PDCs or UCs, recurrence, the acquisition of metastatic properties and/or the development of therapy resistance.

CD97, a G-protein-coupled receptor (GPCR), is normally expressed on cells of hematopoietic origin and smooth muscle but is expressed at very low levels, or is absent in normal epithelial cells.[8,9] Carcinomas derived from various epithelial tissues consistently demonstrate increased CD97 expression compared with normal adjacent tissue.[10–14] CD97 is a member of the adhesion-linked GPCRs, a family of membrane-bound proteins characterized by a large extracellular subunit containing one to a few adhesion motifs noncovalently associated with a conserved GPCR seven-transmembrane domain.[15] To date, a ligand acting through the adhesion domain to mediate CD97 GPCR-dependent signaling has not been identified.[9]

Recently, we have shown that CD97 signals through $G\alpha_{12/13}$ to increase RHO-GTP levels and that CD97 heterodimerizes with lysophosphatidic acid receptor (LPAR), itself a GPCR, potentiating lysophosphatidic acid (LPA)-stimulated RHO activation and RHO-dependent invasion.[14] LPARs are high-affinity cognate receptors for LPA. LPA is produced from complex phospholipids such as lysophosphatidyl choline upon hydrolysis by the enzyme

autotaxin (ATX).[16] LPA binds to LPARs to initiate signaling that mediates a variety of cellular processes including proliferation, survival, cytoskeletal restructuring, and secretion of cellular factors.[16,17] Increased ATX and LPAR expression are correlated with tumorigenesis and progression in various epithelial cancers.[18]

To evaluate whether there is a functional role for CD97 in thyroid cancer progression, we introduced the human 5EGF splice variant of CD97 into the follicular epithelium of $Thrb^{PV/PV}$ mice. The $Thrb^{PV}$ knock-in mouse model possesses a targeted mutation (PV) to the thyroid hormone receptor β-gene locus resulting in complete loss of thyroid hormone (T3) binding,[19] one consequence of which is non-suppressible, elevated levels of thyroid-stimulating hormone.[20] $Thrb^{PV/PV}$ mice spontaneously develop thyroid carcinomas of follicular cells with pathological progression reminiscent of human TFCT.[21–25]

In the present study, we demonstrate that CD97 expression is induced in a majority of clinical thyroid carcinoma samples and that the level of CD97 is further increased in PDCs and UCs relative to co-occurring DTC components. In a mouse model of TFCC, constitutive, transgenic expression of CD97-enhanced LPA and serum-stimulated ERK activation in cultured tumor cells, increased the frequency of pERK- and Ki67-positive cells in tumors, and accelerated the rate of developing lymphovascular invasion and metastasis, supporting a signaling role for CD97 in thyroid cancer progression. Consistent with the known mechanism for CD97 signaling, we show that CD97 heterodimerizes with LPAR in thyroid cancer cell lines, leading to an amplification of LPA-dependent RHOA-mediated invasion. Like CD97, LPAR expression levels were induced in thyroid carcinomas, relative to normal thyroid epithelium.

RESULTS

CD97 is induced in thyroid cancer and its level of expression correlates to malignant grade

We conducted a comprehensive analysis of CD97 expression with respect to a variety of pathological thyroid conditions including hyperplasia, goiter, adenoma, and various categories of carcinoma of follicular cell derivation and metastasis (TMA#1). Immunohistochemical analysis revealed no CD97 expression in normal thyroid epithelium. For neoplastic conditions, membrane, cytoplasmic and occasional nuclear CD97 localizations (Figure 1a) were observed in 56% of adenomas, with increasing frequency of positive cells in FTCs and PTCs (Table 1). There was fairly uniform staining intensity across the tissue cores, although the number of CD97(+) tumor cells varied between the specimens (Table 1). A moderate (>25 to <60% positive cells) to high (⩾60% positive cells) degree of CD97 staining was observed in 69% of FTCs and 100% of non-follicular variants of PTC (non FV-PTCs). This level of CD97 staining (>25% positive cells) was found in only 45% of cases of FV-PTC, which is characterized by a lower rate of lymph node involvement and better prognosis than other variants of PTC.[21] CD97 was expressed in all cases ($n = 8$) of metastasis to the lymph nodes, whereas in a small sample size of distal metastases, CD97 expression was observed in cores from two of three patients.

We also examined a thyroid tissue microarray (TMA#2) containing PDCs and UCs (Table 2). Overall, 93% and 100% of the PDCs and UCs, respectively, disclosed a diffuse,

cytoplasmic and membranous pattern of CD97 expression. More than half (62%) of the positive PDCs (48/77) and 90% of the positive UCs (37/41) featured high-or-moderate staining intensity in⩾60% of the cells present in the tissue cores (Table 2). In contrast to TMA#1, TMA#2 exhibited a range of CD97 staining intensities that were dependent upon the degree of intratumoral dedifferentiation and progression (Figures 1b, c and 2). Twenty-six per cent of the cases analyzed (33/124) displayed adjacent DTC components along with areas of PDC and UC. In these cases, increased intensity of CD97 staining corresponded with areas of intratumoral dedifferentiation and progression (Figures 1b and c, and Figure 2). The staining patterns in the tissue arrays indicate that CD97 is expressed in early stages of thyroid cancer and its expression levels increase with dedifferentiation and progression of disease.

CD97 is expressed in thyroid cancer cell lines and has a role in RHOA activation and LPA-initiated invasion of these cells

To investigate CD97-related signaling in human thyroid cancer, we examined relative expression levels of CD97 in various human thyroid cancer cell lines with known genetic alterations. The panel of cells included those with $BRAF^{V600E}$ mutations and RET/PTC rearrangements commonly observed in PTCs and RAS mutations expressed in PTCs, FTCs, PDCs and UCs.[1,3,22] CD97 expression was detectable in most of these thyroid cancer cell lines but not in immortalized lines from non-neoplastic thyroid. Cell lines such as SW1736, BHT-101 and BCPAP with $BRAF^{V600E}$ mutations consistently expressed the highest levels of CD97 protein (Figure 3a). Inhibition of $BRAF^{V600E}$ activity did not affect CD97 expression (data not shown), implying that $BRAF^{V600E}$ and high levels of CD97 most likely co-occur in these aggressive cancers but that $BRAF^{V600E}$ does not directly regulate CD97 expression. Recently, we have shown in prostate cancer that one mechanism of CD97-dependent signaling results from CD97 heterodimerization with LPA receptor (LPAR) to enhance LPA-dependent signaling through RHOA and ERK.[14] To determine whether this mechanism is operational in thyroid cancer, CD97 was depleted and RHO-GTP levels were measured in two high CD97-expressing (SW1736 and BCPAP) and two low/non-CD97-expressing (CAL62 and NTHY) cell lines. Depletion of CD97 decreased RHOA-GTP levels significantly in SW1736 and BCPAP and minimally in CAL62 following starvation and stimulation with LPA, (Figure 3b). RHO-GTP levels in NTHY, immortalized normal thyroid cells, were barely detectable. Consistent with this effect on RHO-GTP, depletion of CD97 reduced invasion stimulated by LPA or FCS, which contains substantial levels of LPA, to a much greater extent in SW1736 and BCPAP cells than in CAL62 cells. There was little effect on invasion of NTHY cells. By contrast, invasion and RHO-GTP levels stimulated by EGF were unaffected by CD97 expression in all of the cell lines (Figure 3c and Supplementary Figure 1).

RT–PCR was used to determine the composition of LPAR isoforms in the thyroid cell lines shown in Figure 3b. LPARs1–3 were expressed at variable levels in all of the cell lines whereas LPAR 4–6 were expressed in some of the cell lines (Supplementary Figure 2a). Co-immunoprecipitation assays of CD97 with separately transfected LPAR isoforms 1–4 showed that CD97 co-precipitates with LPARs 1, 2 and 3 (data not shown). Because LPAR1 has been shown to promote invasion and proliferation in various cancer cells,[23,24] we

depleted LPAR1 in the four thyroid cell lines. LPAR1 depletion led to cell death in the nontransformed NTHY line, but it was possible to select for LPAR1 depletion in the cancer cell lines (Supplementary Figure 2b). LPAR1 depletion inhibited invasion to LPA and inhibited LPA-stimulated DNA synthesis (Supplementary Figures 2c–f) and cell growth (not shown). By contrast to the inhibitory effect of CD97 depletion on LPA-induced invasion, CD97 depletion alone had a minor effect upon LPA-stimulated DNA synthesis (Supplementary Figures 2d–f). This suggests that there are qualitative or quantitative differences in signaling that mediate invasion in comparison to proliferation downstream of LPARs in these thyroid cancer cell lines. Of interest, depletion of both LPAR1 and CD97 in the cancer cells resulted in cell death, consistent with a synergistic effect of CD97 on LPAR signaling.

Proximity ligation assays demonstrated significant heterodimerization between endogenous CD97 and introduced HA-LPAR1 in BCPAP, SW1736 and to a much lesser extent Cal62 (Figure 3d). In addition, proximity ligation assays performed on cells, following starvation and stimulation with LPA, suggested in Cal62 and SW1736 cells that LPA can potentiate or stabilize the CD97–LPAR interaction, while constitutive heterodimerization occurred in BCPAP (Supplementary Figure 3).

CD97 expression in murine thyroid cancer follows the same pattern as in human disease

Our findings that CD97 promotes LPA-stimulated invasion of thyroid cancer cell lines and that CD97 expression correlates with thyroid tumor dedifferentiation and progression in clinical samples suggested that CD97 may have a role in promoting an aggressive thyroid cancer phenotype. We used a mouse model of TFCC to elucidate the function of CD97 in thyroid cancer development. The $Thrb^{PV}$ model is characterized by elevated levels of circulating TSH and development of follicular thyroid adenoma with eventual progression to carcinoma and metastasis, resulting from the accumulation of additional mutations.[25,26] We assayed CD97 expression in normal thyroid tissue and in tumors arising in $Thrb^{PV/PV}$ animals. As shown in Figure 4, endogenous CD97 is absent in normal mouse follicular epithelium and is clearly detectable in carcinoma. As expected, CD97 was strongly expressed in stromal smooth muscle and endothelial cells observed within thyroid sections. To test our hypothesis that constitutive CD97 expression would accelerate the development of thyroid carcinoma, we engineered a CD97 transgenic mouse constitutively expressing human CD97–5EGF from the bovine thyroglobulin promoter (Figure 5a). The expression of transgenic CD97–5EGF protein, confined to the follicular epithelium, was confirmed by western blot analysis of thyroid tissue lysates and by immunohistochemistry of thyroid tissue sections using an antibody specific for human CD97 (Figures 5b and c).

Constitutive CD97 expression in the follicular epithelium of $Thrb^{PV/PV}$ mice increases the rate of progression to vascular invasion and metastasis and leads to metastatic lesions with a more aggressive histology

The CD97 transgenic line was crossed with the $Thrb^{PV/PV}$ line and tumor progression along with CD97 expression were assessed over time. Normal thyroid, thyroid carcinomas, and invasive tumor cells within the vasculature expressed substantial amounts of transgenic CD97 (Figures 5c–e). Two characteristics of cancer progression, vascular invasion and distal

metastasis, were accelerated in CD97 transgenic mice. Figure 6a shows that constitutive expression of CD97 in the follicular epithelium increased the incidence of vascular invasion (from 33 to 67%) and metastasis (from 12 to 24%). The effect of CD97 on vascular invasion is particularly dramatic in younger mice (24–44 weeks), where the incidence of vascular invasion was increased from 19 to 60% by expression of CD97 (Figure 6b). The increase in vascular invasion was statistically significant as determined by contingency table analysis. Although vascular invasion is a risk factor for the development of metastasis, many of the mice had to be euthanized because of morbidity from the primary tumor before metastatic lesions could be detected in the lungs, resulting in low numbers of mice with metastases. The total number of lung lesions among the eight $Thrb^{PV/PV}$ CD97(+) mice with metastasis was 39 whereas the four $Thrb^{PV/PV}$ CD97(−) mice demonstrated a total of 18 lesions. As shown in Figures 6c and d, constitutive expression of CD97 increased the rate for development of vascular invasion and metastasis to the lungs.

In addition to an increased incidence of metastasis, $Thrb^{PV/PV}$ mice expressing the CD97 transgene displayed lung metastases with a more aggressive phenotype. CD97(+) metastases were mostly extravasated into the surrounding lung parenchyma (Figure 6e) whereas nontransgenic mice had lesions that were either minimally extravasated indicating early metastasis or completely retained in blood vessels as tumor emboli. Seventy-two per cent (28/39) of the total lung metastases in the $Thrb^{PV/PV}$ CD97(+) mice and 28% (5/18) in $Thrb^{PV/PV}$ CD97(−) mice were completely extravasated ($P = 0.0033$). Unexpectedly, lung metastases disclosed very low levels of endogenous CD97 with occasional CD97-stained target cells in $Thrb^{PV/PV}$ CD97 transgenic mice (Supplementary Figure 4) indicating that CD97 is not involved in metastatic colonization *per se*. It is also possible that differences within the lung as compared with the thyroid microenvironment in the mouse may have contributed to the decrease in CD97 expression. Because CD97 was clearly expressed in tumor emboli within the thyroid vasculature and CD97 expression increased the number of lung metastases, it seems that CD97 accelerated the development of invasive thyroid cancer. Cells that eventually colonize the lungs seem to have been further selected for other characteristics unrelated to CD97 expression. We conclude that CD97 promotes cancer progression toward vascular invasion and consequently onset of metastasis. Overall survival was not different between $Thrb^{PV/PV}$ mice with or without the CD97 transgene. The majority of mortality and morbidity was secondary to the compression of the esophagus and trachea by the primary tumor, which occurred as early as 18 weeks and as late as 64 weeks and did not vary significantly with or without transgenic CD97 (Supplementary Figure 5). CD97 transgenic mice lacking the $Thrb^{PV/PV}$ mutation did not develop hyperplasia or show any signs of progression toward abnormal thyroid epithelium indicating that CD97 expression alone was not sufficient to induce transformation in these cells.

CD97 promotes upregulation of signaling pathways in normal thyroid epithelium and thyroid cancer cells

To begin defining the mechanism of CD97 action, we investigated signal transduction pathways relevant to thyroid cancer development and progression. Immunohistochemical analyses were performed on normal (N) thyroid sections taken from animals with and without the CD97 transgene and on tissues at various stages of TFCT from $Thrb^{PV/PV}$ mice

with or without the CD97 transgene. Retarded growth and larger thyroid follicle size were reported for *Thrb*$^{PV/+}$ as compared with wild-type mice.[20] However, on the mixed background of mice used for our studies, there were no apparent differences in animal size or thyroid follicle size between heterozygous (*Thrb*$^{PV/+}$) and wild-type (*Thrb*$^{+/+}$) mice, with or without transgenic CD97.

Tumors were categorized based on the presence or absence of vascular invasion. Proliferation rate was analyzed using the Ki67 marker. Figures 7a and b, show that presence of the CD97 transgene most dramatically increased the percentage of Ki67(+) cells in hyperplasic thyroid and thyroid tumors before the onset of vascular invasion. These data demonstrate a collaborative effect of CD97 and oncogenic signals on thyroid epithelial proliferation. Abnormal proliferation is often accompanied by increased apoptosis, and the percentage of cells displaying cleaved caspase-3 was increased in normal and hyperplasic epithelium (Figure 7c). The combined increase in both proliferation and apoptosis in developing tumors is consistent with no differences in the range of sizes or weights of tumors with or without transgenic CD97 (Supplementary Figure 6).

We have shown previously that one pathway of CD97-initiated signal transduction is via $G\alpha_{12/13}$ to RHOA and ERK.[14] Staining for pERK in normal thyroid or *Thrb*$^{PV/PV}$ thyroids at various stages of TFCC revealed that constitutive expression of CD97 in follicular epithelium increased the level of pERK, even in normal epithelium (Figure 8a). Unscheduled CD97-dependent ERK activation in normal epithelium may have led to the observed increase in apoptosis (Figure 7c). Of interest, thyroid tumors isolated from *Thrb*$^{PV/PV}$ mice expressing transgenic CD97 had numerous clusters of cells with a less differentiated morphology. These cell clusters were rare in comparable CD97(−) tumors. Cells within these clusters, which were interspersed with adenoma/carcinoma, were smaller and rounder in morphology, were located in less differentiated follicular or papillary structures, and were frequently positive for Ki67 (Figure 7b) and pERK staining (Figure 8b). These foci had several morphological hallmarks of increased malignancy including increased nuclear and cellular pleiomorphism, karyomegally, and increased nuclear to cytoplasmic ratio and mitotic rate. AKT, another signaling component that regulates proliferation and apoptosis, has been shown to promote thyroid cancer development and progression in *Thrb*$^{PV/PV}$ mice.[26] Consistent with this, we observed increased pAKT during tumor initiation and development (Figure 8c). However, constitutive CD97 expression did not appear to influence the frequency of pAKT(+) cells. Western blots of whole thyroids verified increased pERK and unchanged pAKT levels in CD97 transgenic thyroids (Figure 8d). Importantly, CD97 transgenic thyroid cancer organoids grown in culture demonstrated enhanced constitutive and LPA-stimulated ERK activation relative to non-transgenic tumor organoids (Figure 8e). In conclusion, transgenic CD97 expression in thyroid follicular epithelium correlated with increased pERK signaling in these cells, implying a direct effect of CD97 expression upon thyroid epithelium. In addition, CD97 expression coincided with a higher proliferative rate in developing tumors and with the presence of pERK(+), Ki67(+) clusters of poorly differentiated tumor cells.

To investigate whether clinical specimens of thyroid cancer demonstrate CD97-associated signal transduction similar to that identified in cell lines and in the *Thrb*$^{PV/PV}$ mouse model,

we analyzed coexpression of CD97 with Ki67, pERK and pAKT in the thyroid cancer tissue microarray (TMA#1) described earlier (Table 1). Spearman's analysis confirmed significant positive correlation (P<0.0001) between CD97 expression and Ki67, pERK and pAKT when comparing normal thyroid epithelial cells and various histotypes of thyroid tumors (Table 3). Analysis of specific categories of progression indicated that, in samples of adenoma and papillary carcinoma (PTC and FV-PTC), CD97 expression positively correlated with pAKT and Ki67. Supplementary Figure 7a demonstrates that the majority of PTC cases in TMA #1 also followed the same pattern for CD97 expression and pERK, with 67% (26/38) of the cases having positive or negative staining for both CD97 and pERK. Specifically, most of the cases (25/38) displayed positive staining for both pERK and CD97. Although the low number of follicular carcinoma specimens did not allow for accurate statistical analysis, the expression patterns between CD97 and pERK or pAKT or Ki67 were usually parallel (Supplementary Figure 7b). Overall these correlation data demonstrate the association between CD97 and other markers of thyroid cancer aggressiveness in genetically heterogeneous thyroid cancers.

To address the potential clinical relevance of our findings that CD97 heterodimerizes with LPAR1 in human thyroid cancer cell lines to potentiate LPA-stimulated RHO activation and invasion, we compared histological staining of LPAR1 and CD97 in a thyroid tissue microarray (TMA#1). Immunohistochemical analysis revealed that LPAR1 was expressed in 86% (6/7) of normal thyroid epithelium cases with predominantly (71%) weak staining and some (14%) moderate staining (Figure 9a and Supplementary Table 1). All PTCs and 92% (12/13) of FTCs expressed LPAR1, and within these DTC samples, 460% of the tissue cores were categorized as intensely stained. Statistical analysis revealed a positive correlation between staining for CD97 and LPAR1 expression in TMA#1 (Spearman coefficient 0.4186, P<0.0001). Immunostaining of normal mouse thyroids ($Thrb^{PV/+}$) and thyroid tumors from $Thrb^{PV/PV}$ mice demonstrated that LPAR1 expression increased significantly in thyroid tumors, similarly to human thyroid cancers. LPAR1 expression was not influenced by the expression of the CD97 transgene (Figure 9b). Co-localization of CD97 and LPAR1 was demonstrated by immunofluorescence in $Thrb^{PV/PV}$ mice (Figure 9c) and in organoid culture of mouse thyroid epithelial cells (Figure 9d).

DISCUSSION

The identification of signaling pathways involved in thyroid cancer progression is critical to facilitate development of therapeutic strategies and improve disease diagnostic and prognostic markers. The need for therapeutics to treat PDCs and UCs is especially profound.[4,6,7] In the present study, we used human thyroid cancer cell lines and a preclinical mouse model of TFCC to gain mechanistic insight into the role that the GPCR, CD97, has in promoting thyroid cancer dedifferentiation and progression. Importantly, we determined that constitutive expression of CD97 in thyroid follicular epithelium significantly accelerated progression to vascular invasion and metastasis in a model of TFCC. The known mechanism of CD97 signaling, through LPAR heterodimerization and LPA-initiated coupling to RHO,[14] occurred in human thyroid cancer cells where depletion of CD97 resulted in decreased LPA-mediated invasiveness. CD97 and LPAR expression increased in association with thyroid cancer progression and these GPCRs demonstrated significant co-expression. Our findings

suggest that the CD97-LPAR-LPA axis should be explored as a therapeutic modality for high-risk and advanced thyroid cancers.

Aberrant expression of CD97 has been demonstrated in several epithelial cancers including 29 thyroid carcinomas.[9] Here, we show, in 263 clinical cases (805 samples) representing various stages of TFCT, that CD97 is absent in normal thyroid, is occasionally expressed in goiters, is expressed in a portion of adenomas, increases in expression with the development of well-differentiated FTCs and PTCs, and increases even further both in numbers of cells and level of expression as tumor cells progress to PDC and anaplasia. The fact that CD97 is expressed in multiple types of carcinomas, including all stages and types of thyroid carcinomas of follicular cell derivation, implies that CD97 induction is not associated with a specific genetic mutation but rather is the consequence of several pro-tumorigenic signaling pathways.

Similarly to carcinoma-induced CD97 expression, LPA receptors ($LPAR_{1–3}$) have a broad tissue distribution.[16] LPAR1 was expressed at relatively low levels in normal thyroid epithelium and benign pathologies, whereas the staining intensity significantly increased with the development of PTCs and FTCs. Increased LPAR levels similarly have been described for other carcinomas including the breast, ovarian, colon and gastric cancers.[16]

Early constitutive expression of CD97 protein in thyroid follicular epithelium of $Thrb^{PV/PV}$ mice significantly accelerated carcinoma progression. Interestingly, we found that transgenic CD97 expression, even in normal thyroid epithelium, resulted in a marked increase in the number pERK + cells, consistent with previously observed CD97-mediated, RHO-dependent ERK activation in prostate cancer cells.[14] Importantly, it was possible to demonstrate in cultured organoids derived from $Thrb^{PV/PV}$ thyroid tumors that serum and LPA stimulation of the ERK pathway was enhanced by transgenic CD97 expression. It is well recognized that activation of the MAPK pathway downstream of common genetic alterations has a major role in thyroid carcinogenesis.[1] In addition, early unscheduled expression of CD97 in $Thrb^{PV/PV}$ mice resulted in increased proliferative indices as assayed by the number of cells expressing Ki67 in developing tumors. Elevated numbers of Ki67 + cells in PTC is considered a risk factor for aggressive disease.[27] In the $Thrb^{PV/PV}$ model, increased levels of pAKT were observed in the earliest epithelial lesions independent of CD97 transgene expression, consistent with a direct effect of the $Thrb^{PV/PV}$ mutation on AKT activation.[28,29] In genetically heterogeneous human thyroid cancers, however, CD97 expression significantly correlated with pAKT immunoreactivity. That CD97-dependent signaling was observed in follicular epithelial cells suggests a direct effect of CD97 expression in TFCC.

Modeling the role of the LPAR-LPA pathway in oncogenesis has suggested that increased LPAR expression collaborates with additional oncogenic events to promote tumorigenesis and progression.[18,30,31] Autocrine signaling dependent upon elevated carcinoma LPAR expression in combination with local ATX expression, leading to LPA production, has been suggested as one mechanism promoting tumor progression.[18,31] Interestingly, increased ATX expression has been described for thyroid UC cell lines and tissue samples.[32] Although LPAR signaling occurs in the absence of CD97, CD97 has a significant effect upon

potentiating downstream RHO and ERK signaling. Therapeutics targeting LPAR signaling are currently being developed.[33] Thus, it will be important to consider the role of CD97 in modulating LPAR function and responses to LPA-LPAR targeted therapies.

In conclusion, CD97 seems to contribute to thyroid cancer aggressiveness as shown by its expression profile relative to thyroid pathogenesis and the promotion of vascular invasion and metastasis in a preclinical model of TFCT. As a GPCR, CD97 is anticipated to be 'druggable' with small molecules. Moreover, its large, antigenic extracellular region may allow antibody directed therapeutics. Taken together, these findings suggest that CD97 should be evaluated as a potential therapeutic target, especially in combination with oncogenic pathway targeting.

MATERIALS AND METHODS

Antibodies and reagents

Rabbit monoclonal antibodies against phosphoAKT1 S473 (pAKT), AKT1, pERK, and cleaved caspase-3 were from Cell Signaling Technology (Beverly, MA, USA). Rabbit polyclonal antibody directed against Ki67 was from Abcam (Cambridge, MA, USA). Anti-α tubulin (DM1A) was from Sigma (St Louis, MO, USA). Anti-HA mouse monoclonal antibody (12C5) was from Roche (Indianapolis, IN, USA). Anti-mouse CD97 goat polyclonal antibody was from R&D Systems (Minneapolis, MN, USA). Anti-human CD97 rabbit polyclonal antibody was as described in Gray *et al.*[8] Anti-LPAR1 (EDG2) rabbit polyclonal antibody (ab23698) was from Abcam. Biotinylated antibodies directed to rabbit, mouse and goat were from Dako North America (Carpinteria, CA, USA).

Histology and immunohistochemistry

Immunohistochemical staining was carried out as before.[14] The numbers of Ki67, pERK, pAKT, and cleaved caspase-3 positive cells were counted in representative 200 × fields and total numbers of cells were quantified using Axiovision software (Zeiss, Thornwood, NY, USA). Eight fields from three separate animals were used to generate the average per cent positive cells.

Thyroid tissue arrays

TMA#1 was generated in the laboratory of Dr Paul Meltzer (139 cases, 257 cores). Because occasional cores were missing from some slides, the core number is not consistent between the CD97 stained specimens and LPAR staining. TMA#2, a tissue microarray containing 124 PDC and UC cases (548 cores) was generated in the laboratory of Dr Ginesa Garcia-Rostan.

Invasion assays

In vitro invasion assays were performed as described in Lagerstrom *et al.*[15]

Proximity ligation assays (DuoLink)

Interaction between LPAR1 and CD97 was determined as described in Ward *et al.*[14]

Statistics

Statistical analyses were done using Prism software.

Supplementary Material

Refer to Web version on PubMed Central for supplementary material.

ACKNOWLEDGEMENTS

This work was supported by the Intramural Research Program, Center for Cancer Research, National Cancer Institute and the Programa Ramón y Cajal—Ministerio de Ciencia e Innovación, Social EU Funds, Universidad de Valladolid, Spain. We acknowledge Barbara J Taylor, Subhadra Banerjee, William G Telford, and Veena Kapoor of the CCR FACS Core Facilities and Christopher D Heger of the CCR Antibody and Protein Purification Unit for their excellent technical support. We thank Drs Cameselle–Teijeiro, X Matías–Guiu, A Herrero and M Fresno–Forcelledo for providing human PDC and UC samples.

REFERENCES

1. Kondo T, Ezzat S, Asa SL. Pathogenetic mechanisms in thyroid follicular-cell neoplasia. Nat Rev Cancer 2006; 6: 292–306. [PubMed: 16557281]
2. DeLellis R, Lloyd RV, Heitz P, Eng C. Pathology and genetics of tumors of endocrine organs WHO classification of tumors. IARC: Lyonpress 2004.
3. Garcia-Rostan G, Sobrinho-Simoes M. Poorly differentiated thryoid carcinoma: an evolving entity. Diagn Histopathol 2011; 17: 114–123.
4. Wiseman SM, Loree TR, Rigual NR, Hicks WL Jr, Douglas WG, Anderson GR et al. Anaplastic transformation of thyroid cancer: review of clinical, pathologic, and molecular evidence provides new insights into disease biology and future therapy. Head Neck 2003; 25: 662–670. [PubMed: 12884350]
5. Sipos JA, Mazzaferri EL. Thyroid cancer epidemiology and prognostic variables. Clin Oncol (R Coll Radiol) 2011; 22: 395–404.
6. Kojic SL, Strugnell SS, Wiseman SM. Anaplastic thyroid cancer: a comprehensive review of novel therapy. Expert Rev Anticancer Ther 2011; 11: 387–402. [PubMed: 21417853]
7. Nagaiah G, Hossain A, Mooney CJ, Parmentier J, Remick SC. Anaplastic thyroid cancer: a review of epidemiology, pathogenesis, and treatment. J Oncol 2011 2011 542358.
8. Gray JX, Haino M, Roth MJ, Maguire JE, Jensen PN, Yarme A et al. CD97 is a processed, seven-transmembrane, heterodimeric receptor associated with inflammation. J Immunol 1996; 157: 5438–5447. [PubMed: 8955192]
9. Yona S, Lin HH, Siu WO, Gordon S, Stacey M. Adhesion-GPCRs: emerging roles for novel receptors. Trends Biochem Sci. 2008; 33: 491–500. [PubMed: 18789697]
10. Aust G, Steinert M, Schutz A, Boltze C, Wahlbuhl M, Hamann J et al. CD97, but not its closely related EGF-TM7 family member EMR2, is expressed on gastric, pancreatic, and esophageal carcinomas. Am J Clin Pathol 2002; 118: 699–707. [PubMed: 12428789]
11. Loberg RD, Wojno KJ, Day LL, Pienta KJ. Analysis of membrane-bound complement regulatory proteins in prostate cancer. Urology 2005; 66: 1321–1326. [PubMed: 16360477]
12. Mustafa T, Eckert A, Klonisch T, Kehlen A, Maurer P, Klintschar M et al. Expression of the epidermal growth factor seven-transmembrane member CD97 correlates with grading and staging in human oral squamous cell carcinomas. Cancer Epidemiol Biomarkers Prev 2005; 14: 108–119. [PubMed: 15668483]
13. Steinert M, Wobus M, Boltze C, Schutz A, Wahlbuhl M, Hamann J et al. Expression and regulation of CD97 in colorectal carcinoma cell lines and tumor tissues. Am J Pathol 2002; 161: 1657–1667. [PubMed: 12414513]
14. Ward Y, Lake R, Yin JJ, Heger CD, Raffeld M, Goldsmith PK et al. LPA receptor heterodimerizes with CD97 to amplify LPA-initiated RHO-dependent signaling and invasion in prostate cancer cells. Cancer Res. [Research Support, N.I.H., Intramural] 2011; 71: 7301–7311.

15. Lagerstrom MC, Schioth HB. Structural diversity of G protein-coupled receptors and significance for drug discovery. Nat Rev Drug Discov 2008; 7: 339–357. [PubMed: 18382464]
16. Lin ME, Herr DR, Chun J. Lysophosphatidic acid (LPA) receptors: signaling properties and disease relevance. Prostaglandins Other Lipid Mediat 2010; 91: 130–138. [PubMed: 20331961]
17. Stortelers C, Kerkhoven R, Moolenaar WH. Multiple actions of lysophosphatidic acid on fibroblasts revealed by transcriptional profiling. BMC Genomics 2008; 9: 387. [PubMed: 18702810]
18. Jonkers J, Moolenaar WH. Mammary tumorigenesis through LPA receptor signaling. Cancer Cell 2009; 15: 457–459. [PubMed: 19477423]
19. Meier CA, Parkison C, Chen A, Ashizawa K, Meier-Heusler SC, Muchmore P et al. Interaction of human beta 1 thyroid hormone receptor and its mutants with DNA and retinoid X receptor beta. T3 response element-dependent dominant negative potency. J Clin Invest 1993; 92: 1986–1993. [PubMed: 8408652]
20. Kaneshige M, Kaneshige K, Zhu X, Dace A, Garrett L, Carter TA et al. Mice with a targeted mutation in the thyroid hormone beta receptor gene exhibit impaired growth and resistance to thyroid hormone. Proc Natl Acad Sci USA 2000; 97: 13209–13214. [PubMed: 11069286]
21. Adeniran AJ, Zhu Z, Gandhi M, Steward DL, Fidler JP, Giordano TJ et al. Correlation between genetic alterations and microscopic features, clinical manifestations, and prognostic characteristics of thyroid papillary carcinomas. Am J Surg Pathol 2006; 30: 216–222. [PubMed: 16434896]
22. Nikiforov YE. Molecular analysis of thyroid tumors. Mod Pathol 2011; 24(Suppl 2): S34–S43. [PubMed: 21455199]
23. Horak CE, Mendoza A, Vega-Valle E, Albaugh M, Graff-Cherry C, McDermott WG et al. Nm23-H1 suppresses metastasis by inhibiting expression of the lysophosphatidic acid receptor EDG2. Cancer Res. [Research Support, N.I.H., Intramural] 2007; 67: 11751–11759.
24. Guo R, Kasbohm EA, Arora P. Sample CJ, Baban B, Sud N, et al. Expression and function of lysophosphatidic acid LPA1 receptor in prostate cancer cells. Endocrinology 2006; 147: 4883–4892. [PubMed: 16809448]
25. Suzuki H, Willingham MC, Cheng SY. Mice with a mutation in the thyroid hormone receptor beta gene spontaneously develop thyroid carcinoma: a mouse model of thyroid carcinogenesis. Thyroid 2002; 12: 963–969. [PubMed: 12490073]
26. Ying H, Suzuki H, Furumoto H, Walker R, Meltzer P, Willingham MC et al. Alterations in genomic profiles during tumor progression in a mouse model of follicular thyroid carcinoma. Carcinogenesis 2003; 24: 1467–1479. [PubMed: 12869418]
27. Kjellman P, Wallin G, Hoog A, Auer G, Larsson C, Zedenius J. MIB-1 index in thyroid tumors: a predictor of the clinical course in papillary thyroid carcinoma. Thyroid 2003; 13: 371–380. [PubMed: 12812214]
28. Lu C, Zhu X, Willingham MC, Cheng SY. Activation of tumor cell proliferation by thyroid hormone in a mouse model of follicular thyroid carcinoma. Oncogene 2011; 9: 12.
29. Saji M, Narahara K, McCarty SK, Vasko VV, La Perle KM, Porter K et al. Akt1 deficiency delays tumor progression, vascular invasion, and distant metastasis in a murine model of thyroid cancer. Oncogene 2011; 30: 4307–4315. [PubMed: 21532616]
30. Lin S, Wang D, Iyer S, Ghaleb AM, Shim H, Yang VW et al. The absence of LPA2 attenuates tumor formation in an experimental model of colitis-associated cancer. Gastroenterology 2009; 136: 1711–1720. [PubMed: 19328876]
31. Liu S, Umezu-Goto M, Murph M, Lu Y, Liu W, Zhang F et al. Expression of autotaxin and lysophosphatidic acid receptors increases mammary tumorigenesis, invasion, and metastases. Cancer Cell 2009; 15: 539–550. [PubMed: 19477432]
32. Kehlen A, Englert N, Seifert A, Klonisch T, Dralle H, Langner J et al. Expression, regulation and function of autotaxin in thyroid carcinomas. Int J Cancer 2004; 109: 833–838. [PubMed: 15027116]
33. Gupte R, Patil R, Liu J, Wang Y, Lee SC, Fujiwara Y et al. Benzyl and naphthalene methylphosphonic acid inhibitors of autotaxin with anti-invasive and anti-metastatic activity. ChemMedChem 2011; 6: 922–935. [PubMed: 21465666]

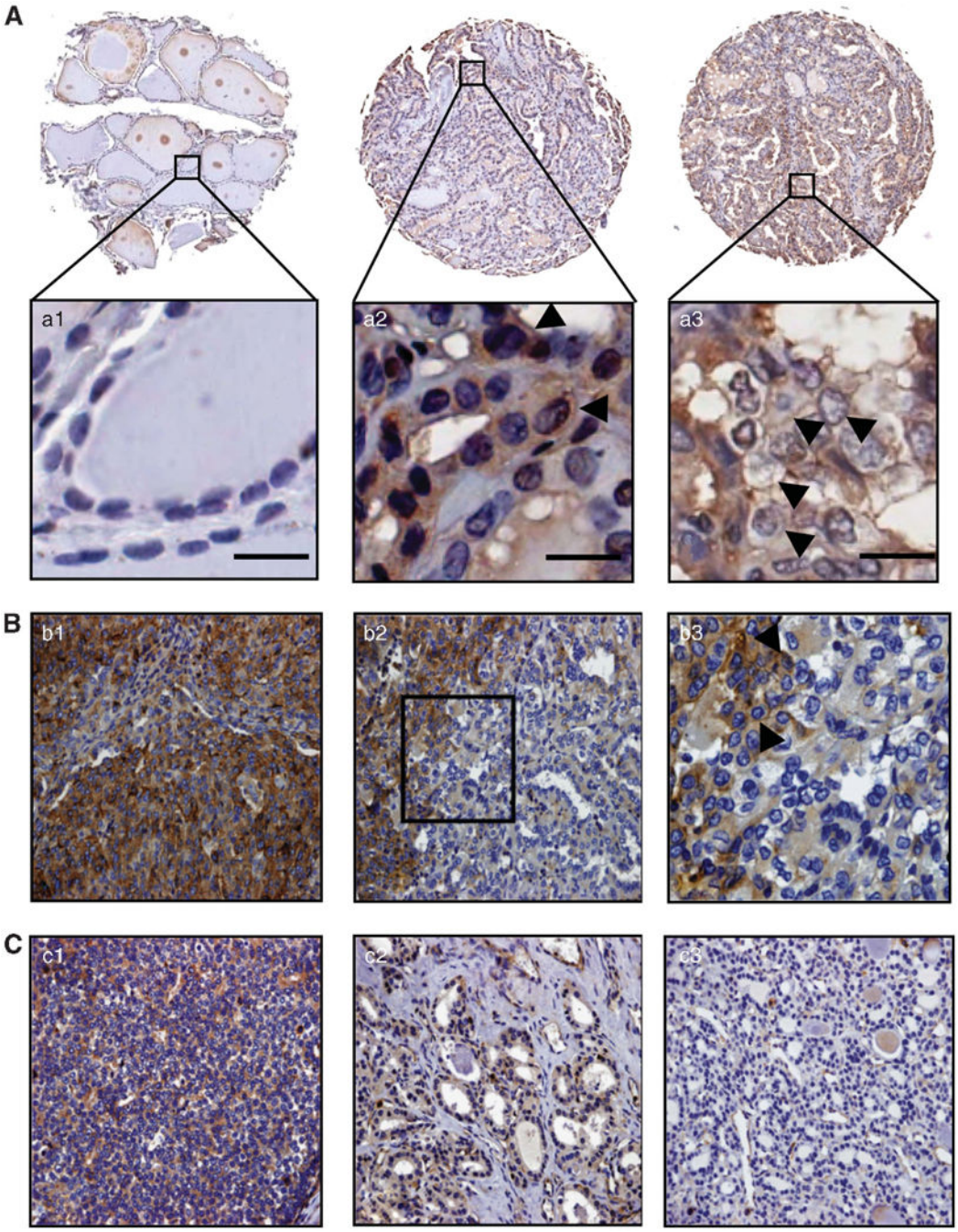

Figure 1.

CD97 is aberrantly expressed in thyroid carcinoma. (**A**) CD97 expression in three representative cores from a human thyroid tissue array (TMA#1). Entire cores and higher magnifications of the areas indicated by the boxes are shown. a1 Normal thyroid negative for CD97; a2 and a3 Primary PTC and lymph node metastasis, respectively, disclosing strong membrane positivity and some cytoplasmic reactivity. Arrows indicate membrane staining. Scale bars, 20 μM (**B**) Intratumoral progression from differentiated FV-PTC to PDC. b1 PDC component showing widespread, strong, cytoplasmic and membrane immunoreactivity.

b2 FV-PTC component (on right) exhibiting primarily moderate cytoplasmic staining and some membrane reactivity dedifferentiating toward PDC (on left). b3 Higher magnification of area framed in B2. Arrows indicate membrane staining. (**C**) Intratumoral progression from differentiated FTC to PDC. c1 PDC component featuring diffuse, intense, cytoplasmic and membrane staining. c2 Invasive front of FTC component displaying distinctive immunoreactivity. c3 Non-invasive front of FTC negative for CD97. (**B**) and (**C**) are representative sections from TMA#2. All tissue arrays were immunostained with a rabbit polyclonal antibody directed against human CD97.

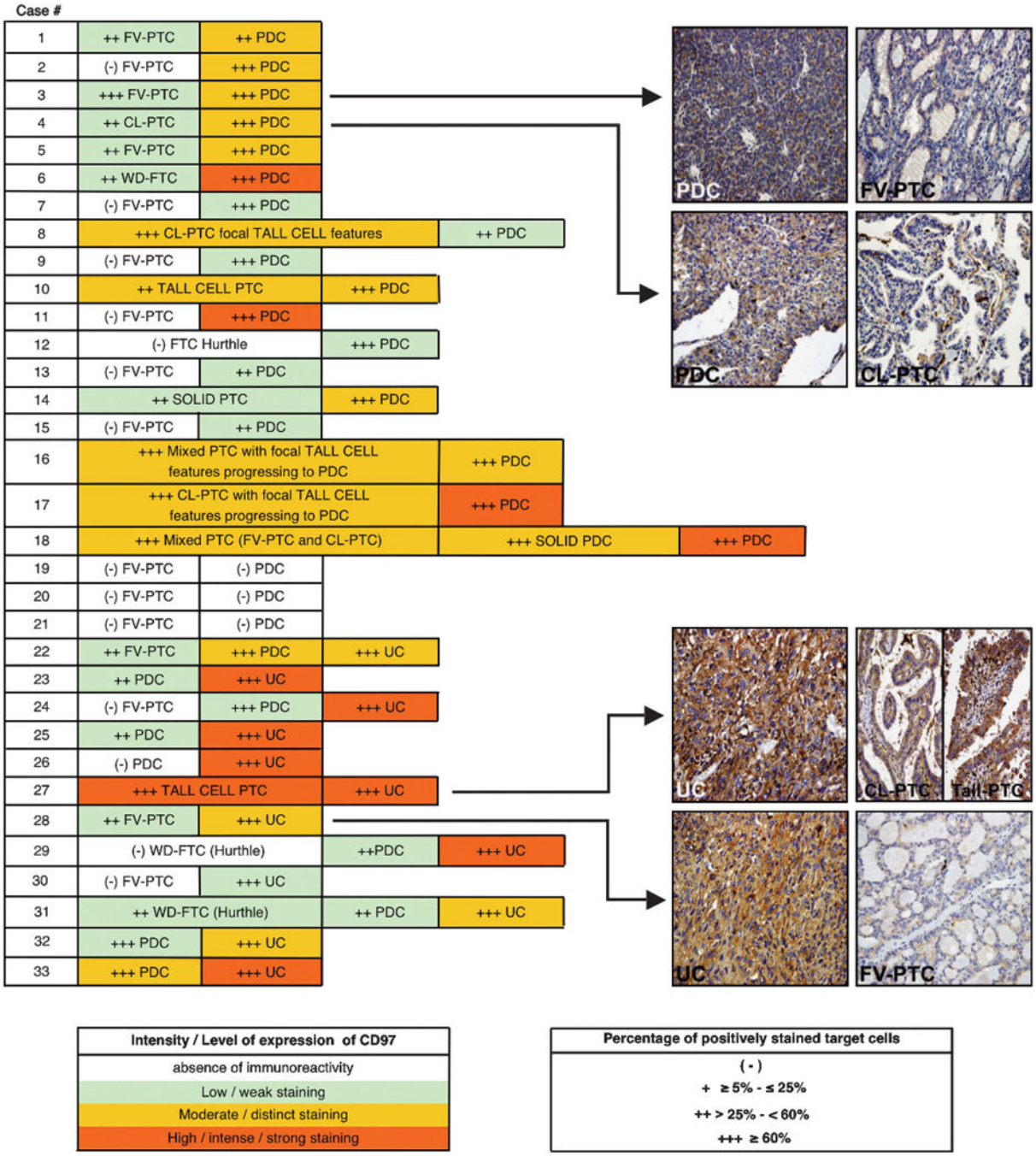

Figure 2.

CD97 expression increases with intratumoral progression in a tissue microarray of PDC/UC thyroid carcinomas (TMA#2). Twenty-six per cent of the PDCs and UCs analyzed (33/124) disclosed a concurrent better DTC component with intratumoral progression/ dedifferentiation. CD97 expression levels in representative tissue cores of cases 3, 4, 27 and 28 are shown. The concurrent better DTC components present within PDCs and UCs included well-differentiated follicular thyroid carcinoma (WD-FTC), follicular variant of

papillary thyroid carcinoma (FV-PTC), classic papillary thyroid carcinoma (CL-PTC), mixed papillary thyroid carcinoma (FV – PTC +CL – PTC), solid PTC, and tall cell PTC.

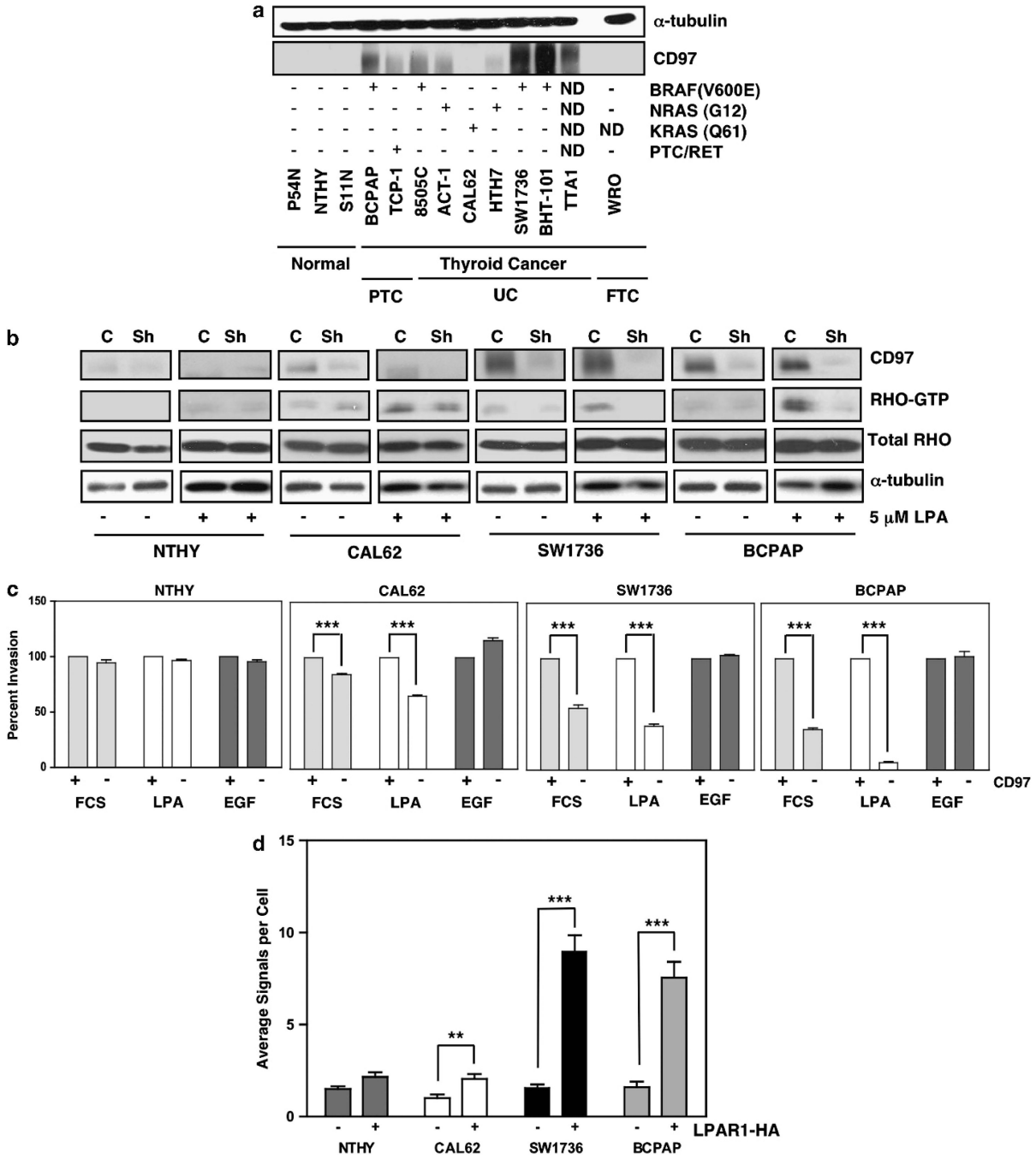

Figure 3.

CD97 expression and function in human thyroid cell lines with known genetic alterations. (**a**) Western blot showing CD97 expression in thyroid cell lines. Genetic mutations for TTA-1 and WRO cells have not been completely characterized (**b**) Western blots showing CD97 expression and RHO-GTP following starvation and stimulation with 5 μM LPA in four human thyroid cell lines. Data is shown for parental cells (C) and cells with depleted CD97 (Sh). (**c**) *In vitro* invasion of thyroid cell lines to FCS (10%), LPA (1 μM) or EGF (25 ng/ml). (**d**) Human thyroid cell lines permanently transfected with empty vector (−) or

LPAR1-HA (+) were subjected to *in situ* proximity ligation assays. Results were quantified using the Duolink Image Tool software. Average of three independent experiments is shown. Error bars represent ±s.e.m. ***$P<0.0001$, **$P<0.001$ at a 95% confidence interval.

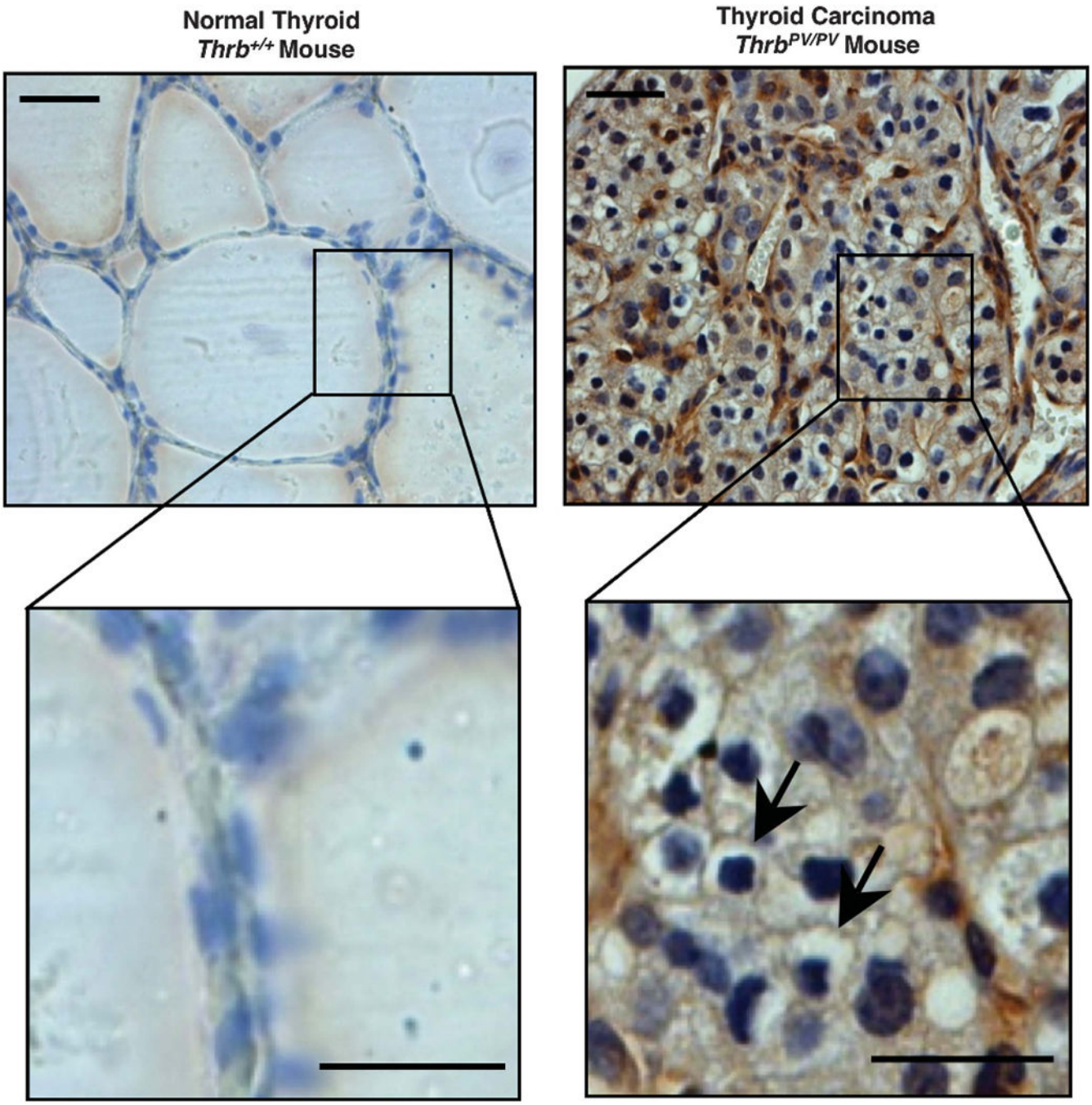

Figure 4.

Mouse CD97 expression increases during progression from normal thyroid to carcinoma. Immunohistochemistry using a polyclonal antibody directed against mouse CD97 was used to demonstrate relative levels of CD97 in normal and malignant thyroid tissue. Boxed regions are shown at higher magnification. Arrows indicate tumor cells with primarily membrane staining and some cytoplasmic expression of CD97. Note high expression of CD97 in stromal smooth muscle and endothelial cells intermingled with tumor cells. Scale bars, 20 μM.

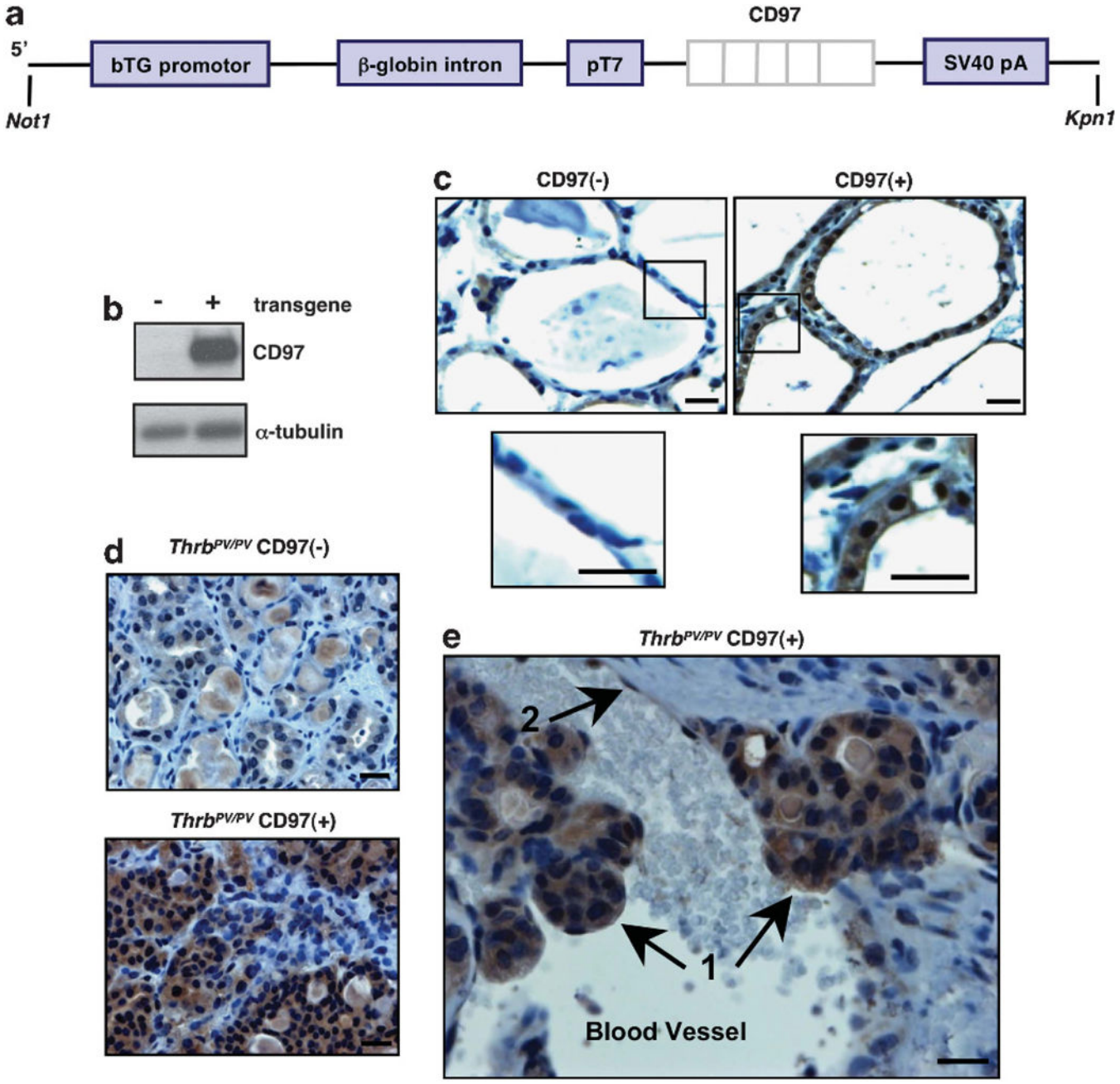

Figure 5.

Generation of a CD97 transgenic mouse model constitutively expressing human CD97 in thyroid follicular epithelial cells. (**a**) A construct containing the human CD97–5EGF cDNA clone downstream of the thyroglobulin promoter was generated. (**b**) Western blot showing expression of human CD97 protein in transgenic mouse thyroid. (**c**) Immunostaining of normal and CD97 transgenic mouse thyroid. Boxed regions are shown at higher magnification. (**d**) Immunostaining demonstrates transgenic CD97 expression in thyroid carcinoma of *Thrb*$^{PV/PV}$ mice. (**e**) CD97 expression in cells that have invaded the vasculature in a *Thrb*$^{PV/PV}$ CD97(+) mouse. Arrows indicate tumor cells (1) and

endothelial cell lining the blood vessel (2). Western blot analysis and immunostaining were performed using a rabbit polyclonal antibody directed against human CD97. Representative sections are shown. Scale bars, 20 μM.

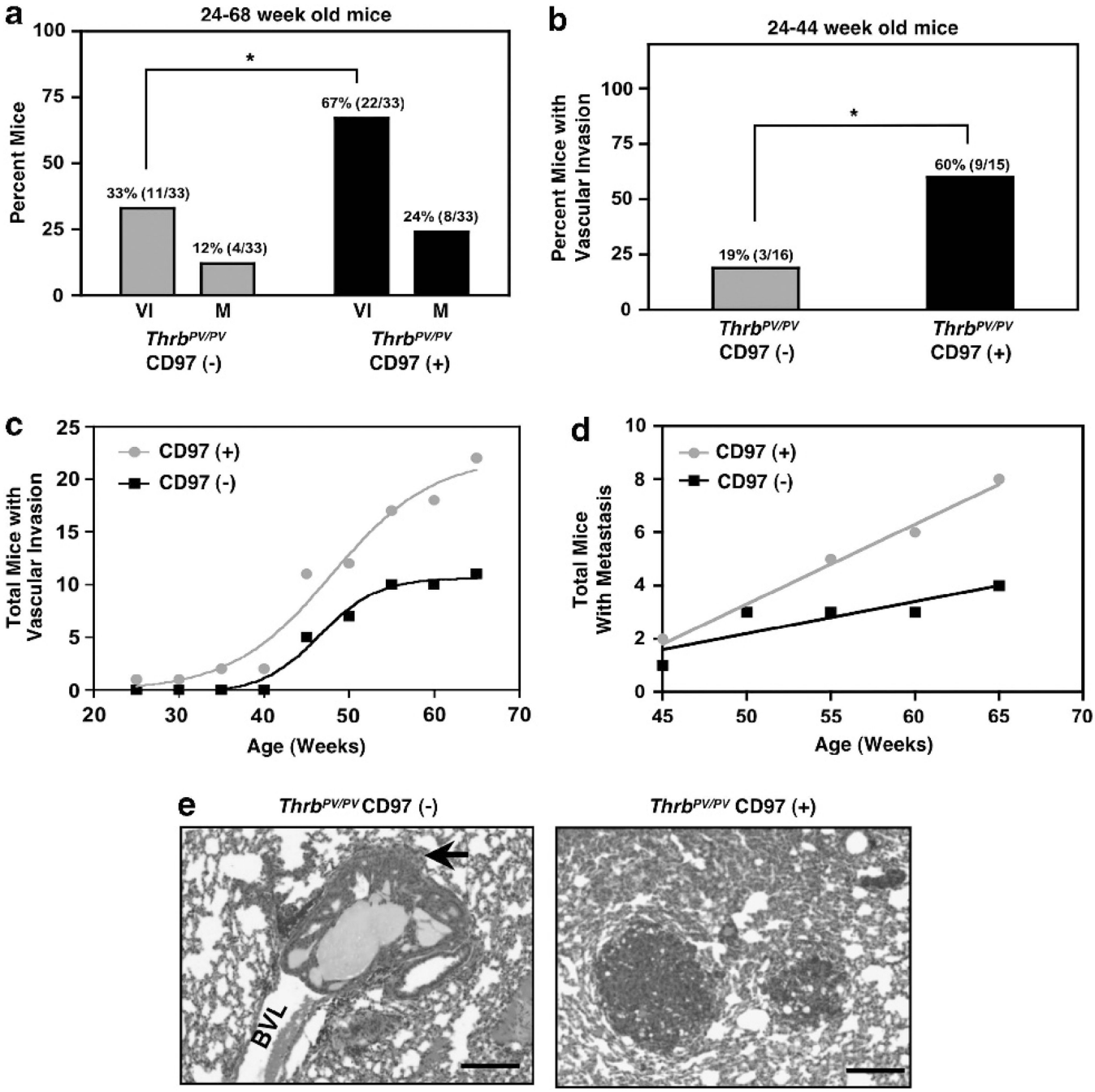

Figure 6.

Thrb$^{PV/PV}$ mice expressing constitutive hCD97 display more rapid progression to carcinoma and develop metastatic lesions with a more aggressive phenotype than control animals. (**a**) Relative incidence of vascular invasion (VI) and metastasis (M) in mice expressing transgenic CD97 compared with control mice. Data shown are from 33 transgenic mice and 33 controls, $*P = 0.0132$. Actual numbers of positive animals shown in parentheses. (**b**) Relative occurrence of vascular invasion in mice between the ages of 24 and 44 weeks. Data shown are based on 15 transgenic and 16 control mice, $*P = 0.029$. Actual numbers of

positive animals shown in parentheses. (**c**) Rate of developing vascular invasion was determined by the cumulative number of mice displaying tumor cells in blood vessels. The two curves are significantly different, $P = 0.005$. (**d**) Rate of occurrence of metastasis is shown as the cumulative number of mice with lung metastasis. The slopes of the two lines are significantly different, $P = 0.007$. (**e**) H&E staining of representative metastatic lesions. Note minimal extravasation of CD97(−) cells (indicated by arrow) from the blood vessel lumen (BVL) Scale bars, 50 μM. Eight CD97(+) mice had a combined number of 39 metastatic lesions and four CD97(−) mice demonstrated a total of 18 lesions.

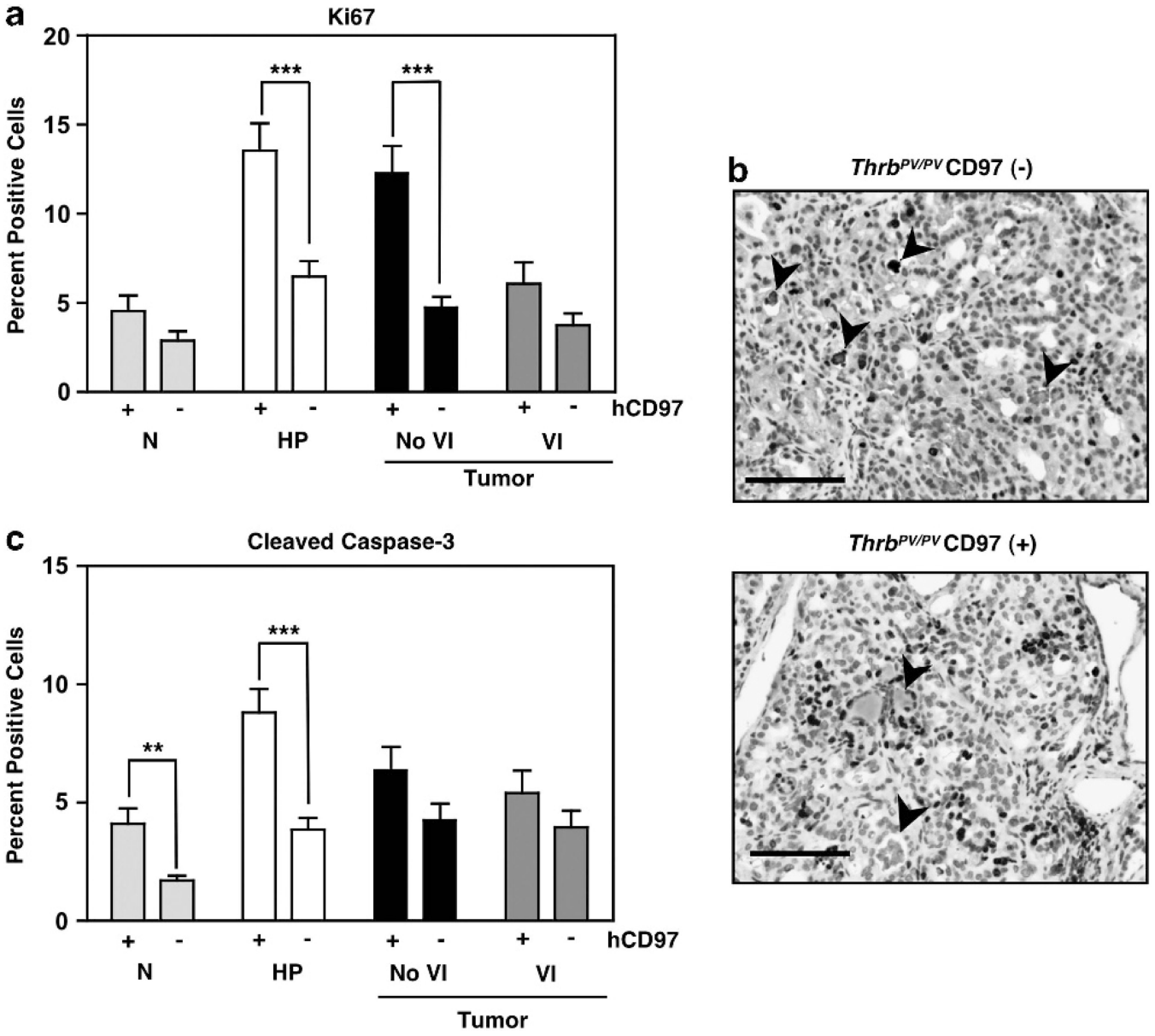

Figure 7.

CD97 transgenic mice display increased Ki67 and cleaved caspase-3. (**a**) Per cent cells expressing Ki67 in normal thyroid (N), hyperplasia (HP), and tumors with or without vascular invasion (VI). Error bars represent s.e.m. ***P<0.0001, **P<0.001, at a 95% confidence interval. (**b**) Representative histology showing increased number of Ki67(+) cells in thyroid carcinoma of $Thrb^{PV/PV}$ CD97(+) mice. Tissue sections shown are from 53-week-old mice. Note areas of colloid staining indicated by arrowheads. Scale bars, 50 μM. (**c**) Per cent cells expressing cleaved caspase-3 as for Ki67 in (A). The tissues were collected from mice at 7–68 weeks (N), 7–9 weeks (HP), 51–68 weeks (No VI), and 45–61 weeks (VI).

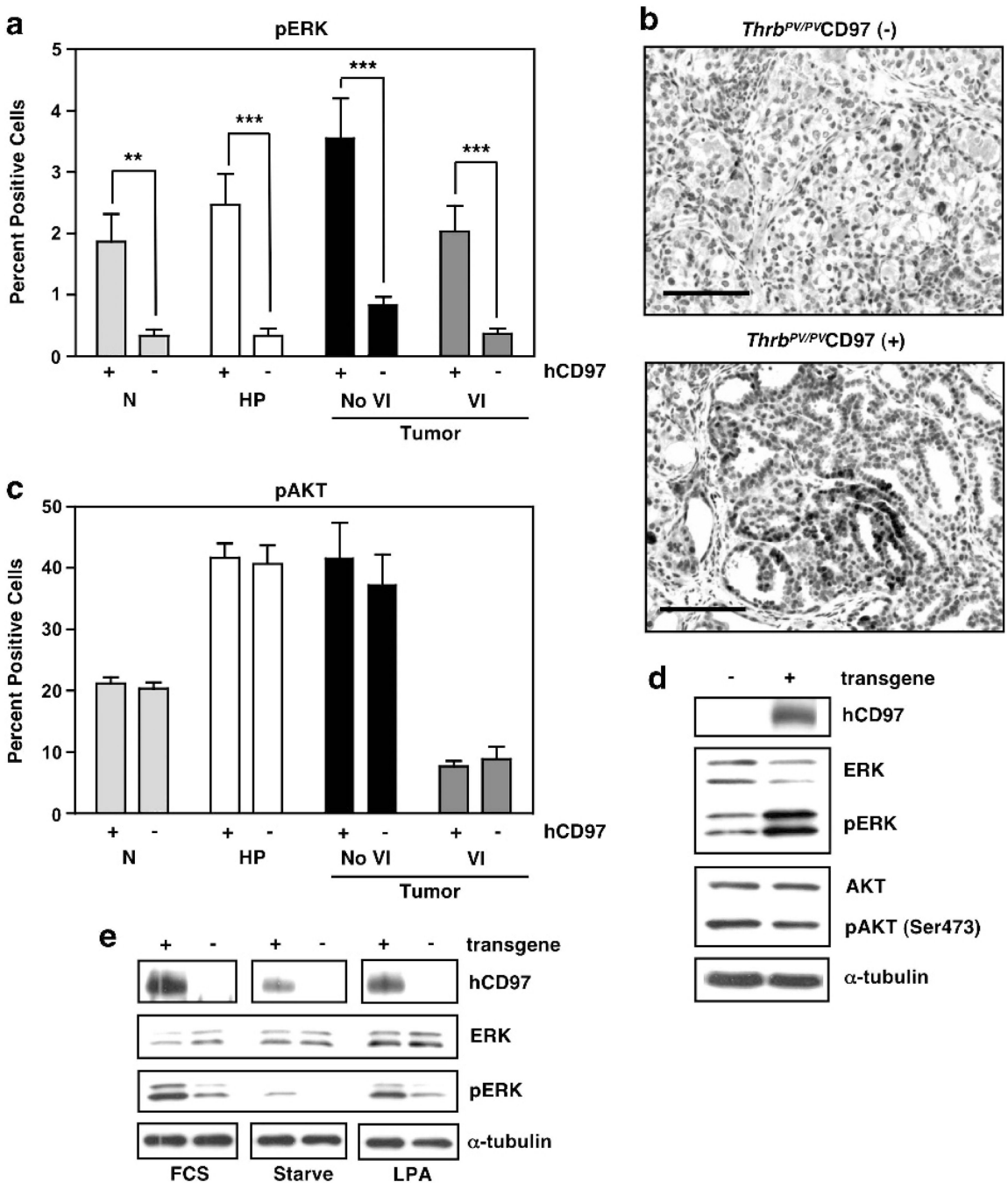

Figure 8.

Constitutive expression of CD97 in follicular epithelium leads to increased phosphoERK. (**a**) Relative numbers of cells with pERK in normal thyroid (N), hyperplasia (HP), and tumors with or without vascular invasion (VI) were determined by immunostaining with anti-pERK rabbit monoclonal antibody. Error bars represent s.e.m. ***P<0.0001, **P<0.001, at a 95% confidence interval. (**b**) Representative sections displaying pERK staining. Note pERK staining was predominantly nuclear with some weak cytoplasmic staining. Tissue sections shown are from 53-week-old mice. Scale bars, 50 μM (**c**) Per cent

cells expressing pAKT was identified using anti-pAKT rabbit monoclonal antibody. The tissues were collected from mice at 7–68 weeks (N), 7–9 weeks (HP), 51–68 weeks (No VI), and 45–61 weeks (VI). (**d**) Western blot analysis of whole thyroids from *Thrb*$^{+/+}$ CD97 transgene (−) or (+) mice. (**e**) Western blot demonstrating ERK phosphorylation in organoid cultures of thyroid epithelial cells. Cells isolated from thyroid tumors of 24 week old *Thrb*$^{PV/PV}$ CD97 transgene (+) or (−) mice were grown in 10% FCS (FCS), starved for 24 h (Starve) or starved for 24 h and stimulated with 1 μM LPA for 10 min (LPA).

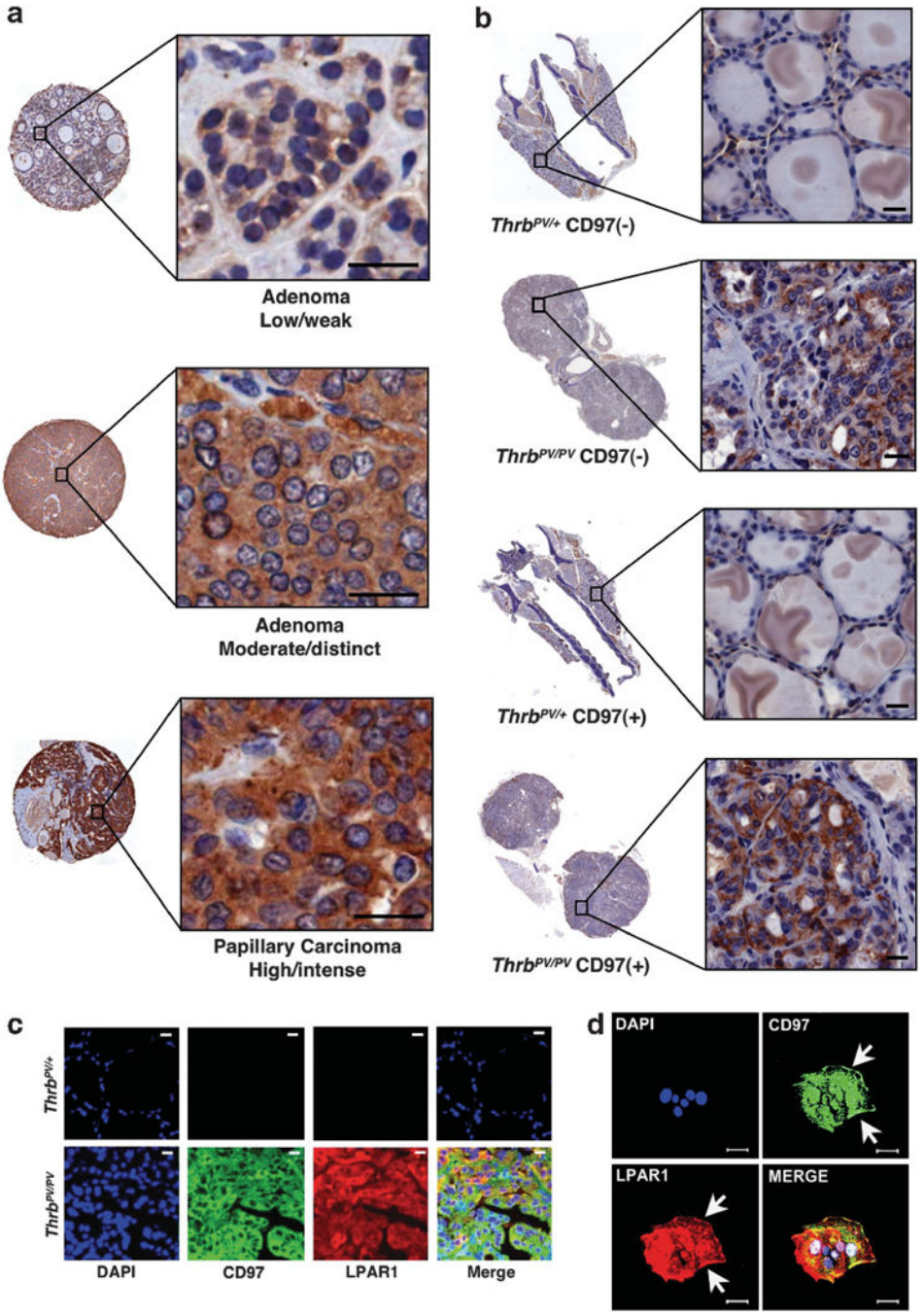

Figure 9.

LPAR1-staining intensity increases with malignant grade in human and mouse tissues. (**a**) LPAR1 staining in three representative cores from a human thyroid tissue array (TMA#1). Entire cores and higher magnifications of the areas indicated by the boxes are shown. (**b**) LPAR1 expression in thyroids from 45-week-old mice. *Thrb*$^{PV/+}$ appeared normal and *Thrb*$^{PV/PV}$ displayed advanced tumors. Entire thyroid sections are shown with higher magnifications in boxes. A rabbit polyclonal antibody directed against LPAR1 was used for immunostaining. (**c**) CD97 co-localizes with LPAR1 in mouse thyroid tumor cells. Normal

mouse thyroids (*Thrb*$^{PV/+}$) and thyroid tumors (*Thrb*$^{PV/PV}$) were stained with goat polyclonal antibody directed against mouse CD97 and rabbit polyclonal antibody directed against LPAR1. (**d**) Epithelial cell organoids grown from mouse thyroid tumors display co-localization of CD97 and LPAR1. Antibodies used were the same as those used in **(c)**. Arrows indicate co-localization of CD97 and LPAR1 on cell membrane. Scale bars, 20 μM.

Table 1.

CD97 expression in normal human thyroid, benign thyroid pathologies, malignant, well-differentiated thyroid carcinomas of follicular cell origin, and metastases (TMA #1)

Diagnosis	Percentage of cells expressing CD97			
	≥60%	>25 to <60%	≥5 to ≤25%	Negative
Normal thyroids (8 cases, 14 cores)	0	0	0	8 (100)
Goiters (17 cases, 31 cores)	0	2 (11.8)	1 (5.9)	14 (82.3)
Hyperplasias (3 cases, 6 cores)	0	0	0	3 (100)
Adenomas (48 cases, 90 cores)	1 (2.0)	17 (35.4)	9 (18.8)	21 (43.8)
Follicular carcinomas (13 cases, 23 cores)	4 (30.8)	5 (38.4)	2 (15.4)	2 (15.4)
Papillary carcinomas (19 cases, 33 cores)	6 (31.6)	13 (68.4)	0	0
Follicular variant papillary carcinomas (20 cases, 39 cores)	1 (5.0)	8 (40.0)	6 (30.0)	5 (25.0)
Local metastases to lymph nodes (8 cases, 15 cores)	1 (12.5)	6 (75.0)	1 (12.5)	0
Distal metastases (3 cases, 6 cores)	0	1 (33.3)	1 (33.3)	1 (33.3)

Numbers in parentheses indicate percentages of cases. Two-tailed Fisher's exact probability test of CD97 expression profiles: Upregulation of CD97 from normal thyroid to non-malignant lesions (goiter, hyperplasia and adenoma) is significant, $P = 0.0191$. Upregulation of CD97 from non-malignant lesions to carcinomas (FTC, PTC, and FV-PTC) is significant, $P < 0.0001$. There is no significant difference between CD97 expression in metastatic lesions and carcinomas, $P = 1.0$. For the statistical analysis, cases were considered positive for CD97 if the per cent of positive cells was ⩾5%.

Table 2.

CD97 expression in highly aggressive, poorly differentiated (PDC) or undifferentiated (UC) thyroid tumors (TMA #2)

Diagnosis	Percentage of cells expressing CD97			
	≥60%	>25 to <60%	≥5 to ≤25%	Negative
PDC (83 cases, 356 cores)[a]	61 (73.5)	15 (18.1)	1 (1.2)	6 (7.2)
UC (41 cases, 192 cores)[a]	39 (95.0)	1 (2.5)	1 (2.5)	0
PDC + UC (124 cases, 548 cores)[a]	100 (80.6)	16 (12.9)	2 (1.6)	6 (4.8)

There is not a significant difference between the CD97 expression profile in PDCs and UCs. $P = 0.1766$ (two-tailed Fisher's exact probability test). The numbers in parentheses indicate percentage of cases. Cytoplasmic staining was present in all positive cases except one PDC, which displayed only membranous immunoreactivity. Both PDC and UC cases showing cytoplasmic CD97 also disclosed different levels of continuous or discontinuous, weak/distinct/strong membranous staining.

[a]To improve the representativity of the expression, analysis two-to-six core biopsies of 1 mm in diameter from different regions of the same specimen or different blocks of the same tumor, were included in the TMAs. (192 tissue cores in the TMA of UC and 365 cores in the TMAs of PDC). Whenever a concurrent better differentiated component or area with different degrees of aggressiveness and/or pattern of growth was observed within a particular tumor, representative tissue cores from those areas were included in the analysis. In a few cases, the primary tumor and the recurrence and/or metastasis were also included.

Table 3.

Correlation between CD97 expression and pERK, pAKT, and Ki67 expression in human samples representing normal thyroids, benign thyroid pathologies, malignant, well-differentiated thyroid carcinomas of follicular cell origin, and metastases (TMA #1)

Diagnosis	Spearman correlation coefficient		
	CD97/pERK	CD97/pAKT	CD97/Ki67
Adenomas (47 cases)	0.2285	0.6148***	0.5864***
Papillary carcinoma (39 cases)	−0.03465	0.4745**	0.6794***
All cases in TMA #1	0.3244***	0.6464***	0.7168***

Spearman correlation coefficients were calculated with a two-tailed *P*-value and a 99% confidence interval.

** $P<0.01$,

*** $P<0.0001$. Percentage of cells expressing pERK, pAKT or Ki67 was scored as for CD97 in Table 1. Papillary carcinomas included PTC and FV-PTC.